Vertical distribution of algal productivity in open pond raceways

Thomas E. Murphy[1,*], Bennett J. Kapili[2], Angela M. Detweiler[1], Brad M. Bebout[1], and Leslie E. Prufert-Bebout[1]

Abstract

In this paper we report a method for experimental measurement of photosynthetic productivity as a function of simulated depth in open pond raceways for algae cultivation. Knowledge of the depth dependence of photosynthetic productivity aids in designing ponds with optimal depth with respect to biomass productivity and capital and operating costs. To simulate depth, we (i) measured irradiance attenuation coefficients of liquid algal cultures as a function of wavelength in the range of 400 to 700 nm, (ii) reproduced the magnitude and spectral content of the irradiance that would exist at various depths within open ponds using a programmable LED array, and (iii) measured photosynthetic rate as oxygen evolution under irradiances corresponding to various depths. We report the depth distribution of photosynthetic rate in simulated 20 cm deep ponds of the green alga *Chlorella vulgaris* and and the cyanobacterium *Spirulina platensis* at a biomass concentration of

[*]thomasemurphy@utexas.edu; 650-604-3826; NASA Ames Research Center, Mail Stop 239-4, P.O. Box 1, Moffett Field, CA 94035-0001

[1]Exobiology Department, NASA Ames Research Center - Moffett Field, CA 94035, USA

[2]Department of Earth and Atmospheric Sciences, Cornell University, Ithaca, NY 14850, USA

0.19 grams dry biomass per liter (g/l). Under an incident irradiance corresponding to full sunlight, the compensation depth for *Chlorella* was 12 cm. Below this depth, net oxygen consumption due to respiration had a magnitude equal to 15% that of the total oxygen production above the compensation depth. For *Spirulina*, negative net oxygen production was not observed at any depth, but the top 13 cm of the pond accounted for 90% of its total oxygen production. These productivity cross sections, in addition to knowledge of the dependence of capital and operating costs on pond depth, enable the design of open ponds for optimal depth for maximum return on investment.

Keywords:

open ponds, raceways, light attenuation, irradiance, light spectra, photosynthesis

---

Nomenclature

A	attenuation cross section, $\mathrm{mm}^{-1}/(\mathrm{g/l})$
a	action spectrum value
C	concentration, mol/l
d	pond depth, m
h_b	box thickness, m
$k_l a$	transfer coefficient, s^{-1}
G	irradiance, μmol photons/m^2
P	pressure, Pa
S	spectral matching parameter
t	time, s

v	velocity, m/s
$\dot{W}$	power consumption, W
w	width, m
X	biomass density, g/l
z	local depth, m
Greek symbols	
α	irradiance attenuation coefficient, mm^{-1}
λ	wavelength, nm
π	production rate, mol/l-s
Subscripts	
h	refers to headspace
i	refers to initial
O_2	refers to oxygen
p	refers to spectrum reconstruction
Abbreviations	
OD	optical density
PAR	photosynthetically active range, 400 to 700 nm
PU	photosynthetically useful

1. Introduction

Open pond raceways provide a low cost platform for cultivating algae for nutritional supplements [1, 2], agricultural and aquacultural feed [3–5], and biofuel feedstock [6–9]. Most open pond raceways consist of an oval shaped pond with a median separator such that fluid is circulated along the 'track'

[10–13]. A paddle wheel is usually used to sustain this circulation. The resultant mixing prevents settling, diminishes vertical gradients of nutrients, carbon dioxide, and oxygen, and also moves cells into and out of the photic zone [14].

Typically, open ponds are about 20 to 30 cm deep [13], which represents a compromise between areal productivity and hydraulic limitations [10, 12]. Areal productivity is inversely related to pond depth because shallower ponds have a greater depth averaged irradiance [11, 15]. Shallower ponds also reduce operating costs by reducing the total volumetric flow rate that needs to be sustained by the paddle wheels. Moreover, shallower ponds have been shown to increase the maximum achievable biomass density [15], which decreases harvesting costs [16]. On the other hand, the maximum achievable track length is proportional to pond depth because the amount of hydraulic head that the paddle wheel can provide is proportional to the height of the water column it can lift. Longer raceways decrease capital costs for hectare-scale algal farms by reducing the total number of raceways that need to be built to cover a prescribed total footprint area.

Optimizing pond depth with respect to these competing effects requires knowledge of the depth dependence of photosynthetic productivity. It is typical to report pond productivity in grams dry biomass per square meter of footprint area per day [6, 13, 17], but this metric neglects the non-uniformity of productivity with depth. Quantification of this non-uniformity enables calculation of overall productivity for different pond depths, which in turn enables quantitative optimization of pond depth for high productivity and low capital and operating costs.

Direct measurement of the vertical distribution of open pond productivity, or photosynthetic rate, is experimentally difficult. At the laboratory scale, photosynthetic rate is often measured as the time rate of change in dissolved oxygen concentration of a closed algal suspension after an illuminating light is switched on [18, 19]. This technique cannot be applied to real ponds because diffusion and advective mixing make it very difficult to recover the local oxygen generation rate from the local oxygen concentration. Alternatively, a modeling approach can be taken for understanding the depth dependence of photosynthetic productivity in ponds [20]. However, it is difficult to accurately take into account the effect of a depth dependent irradiance spectrum on local productivity.

In this study, we present experimentally measured photosynthetic rates as a function of simulated depth within an open pond raceway. To simulate depth, we constructed irradiance spectra that cells would experience at different depths. First, we measured spectral irradiance attenuation coefficients in miniature ponds of the green alga *Chlorella vulgaris* and the cyanobacterium *Spirulina platensis*. Based on these attenuation coefficients, we used a programmable LED array to simulate the irradiance spectra that cells would experience at different depths in these ponds under full sunlight. For each simulated depth, we measured the photosynthetic rates of these species as rates of oxygen production. In this way, we were able to measure a productivity cross section of a simulated open pond, taking into account variation in both the magnitude and the spectral content of irradiance with depth.

2. Materials and Methods

2.1. Stock culture cultivation

The green alga *Chlorella vulgaris* (UTEX 2714) and the cyanobacterium *Spirulina platensis* (ATCC 29408) were used in this study. *Chlorella vulgaris* is a spherical green alga approximately 10 μm in diameter [21]. It contains the pigments chlorophyll a, with absorption peaks at 440 nm and 680 nm, chlorophyll b, with peaks at 470 and 660 nm, and carotenoids, with a broad absorption band between 450 and 500 nm [22, 23]. *Chlorella vulgaris* is of interest in the biofuels market due to its high lipid productivity [24], as well as in the health food market due to its richness in protein, vitamins, polysaccharides, and polyunsaturated fatty acids [25, 26]. Henceforth, *Chlorella vulgaris* will be referred to simply as *Chlorella*.

Spirulina platensis is a cylindrical cyanobacterium about 6 to 12 μm in diameter that forms spiral-shaped filaments tens to hundreds of cells in length [27]. It contains chlorophyll a and carotenoids. Additionally, light harvesting is accomplished by the phycobilisome, which consists of the phycobiliproteins phycocyanin and allophycocyanin [28], which absorb maximally at 620 nm and 650 nm, respectively [29, 30]. *Spirulina* has been eaten by humans for centuries due to its high concentration of protein and vitamins [27, 31]. For several decades, *Spirulina* has been cultivated at large scale in open ponds for sale as a nutritional supplement, with Earthrise® Nutritionals being the world's largest producer. Henceforth, *Spirulina platensis* will be referred to simply as *Spirulina*. Although *Spirulina* is a cyanobacterium, henceforth both *Chlorella* and *Spirulina* will be referred to as 'algae,' as is common practice in the mass cultivation industry.

Stock cultures of *Chlorella* and *Spirulina* were grown in the freshwater medium BG11 (ATCC medium 616) and the *Spirulina* medium proposed by Schlösser [32], respectively. Aliquots containing 1 ml of culture were used to inoculate 100 ml of nutrient media in 250 ml Erlenmeyer flasks. The flasks were placed in an approximately 2 cm deep water bath which was maintained at 25^oC by a chiller (AquaEuroUSA, MC-1/2HP). The cultures were sparged with ambient air passed through a 0.2 μm filter at a rate of 30 ± 20 ml/min. The pH of the cultures was not controlled. Cultivation occurred in a greenhouse on the roof of Ames Research Center (Moffett Field, CA) between August 29 and September 23, 2014. The greenhouse panels were made from acrylite OP4, which has a transmittance of about 92% throughout the ultraviolet, visible, and infrared range of the spectrum [33]. The cultures were not otherwise shaded.

2.2. Measurement of biomass density

In this study, biomass density X is reported in grams dry biomass per liter (g/l). Optical density at 750 nm (OD_{750}) was used as a proxy for biomass because relatively less time and culture volume are required to measure this parameter. Thus, calibration curves were generated between biomass density and OD_{750} for *Chlorella* and *Spirulina*. For this, the OD_{750} of 1x, 2x, 4x, and 8x dilutions of stock culture were measured in a plate reader spectrophotometer (Molecular Devices, SpectraMax M5). Then, 50 ml of the same stock culture was centrifuged. The supernatant was discarded and the cells were rinsed with water and centrifuged again. The supernatant was again discarded, and the biomass was dried in an oven overnight at 80^oC. The dry biomass was then weighed, and the biomass density was calculated

by dividing the biomass by the initial culture volume. It was assumed that the dilutions had biomass concentrations in accordance with their dilution ratios. A least squares regression line was then fitted to the data of biomass density versus OD_{750}. The biomass density of *Chlorella* could be expressed as $X_{Chl} = 0.539 OD_{750}$, with an R^2 value of 0.998 for values of OD_{750} less than 0.7. The biomass density of *Spirulina* could be expressed as $X_{Spir} = 1.39 OD_{750}$ with an R^2 value of 0.999 for values of OD_{750} less than 1.0. At higher optical densities, the relationship between OD_{750} and biomass density became nonlinear due to multiple scattering. Thus, when measuring the OD_{750} as a proxy for biomass in the following experiments, the culture was diluted until its OD_{750} was less than 0.7 and 1.0 for *Chlorella* and *Spirulina*, respectively.

2.3. Photosynthetic rate as a function of simulated depth

Photosynthetic rate was measured as a function of illumination by irradiance spectra that would occur at different depths within open ponds of *Chlorella* and *Spirulina*. The depth dependent irradiance spectra were determined by measuring the irradiance attenuation coefficient as a function of wavelength for each strain. We then calculated irradiance spectra for depths ranging from 0 to 20 cm within each culture given an incident solar irradiance provided by a standard reference [34]. We then reproduced these spectra using a programmable LED array with 16 different color LEDs (TeleLumen, Light Replicator) [33]. Finally, we measured the photosynthetic rate of small volumes of algal culture exposed to irradiance fields whose magnitude and spectral content corresponded to discrete depths. In their totality, these data comprise the "simulated pond."

Hereafter, the irradiance within a narrow spectral band (1.3 nm) will be referred to as the "spectral irradiance." Further, the irradiance as a function of wavelength over a larger spectral range (400 to 700 nm) will be referred to as the "irradiance spectrum."

2.3.1. Measurement of spectral irradiance attenuation coefficients

The local spectral irradiance, $G_\lambda(z)$, is defined as the downwelling component of the directional radiance, integrated over all downward-facing directions, within a narrow bandwidth around wavelength λ, at depth z. In practice, local photosynthetic rate is controlled by the upwelling, in addition to downwelling, irradiance. However, in optically thick ponds where bottom reflection is negligible, the upwelling irradiance is small, on the order of about 1% of the downwelling irradiance. We built a custom experimental setup to measure the attenuation of downwelling spectral irradiance with depth in cultures of *Chlorella* and *Spirulina*. In this setup, a 10 ml sample of stock culture was placed in a 1.9 cm deep, 2.5 cm square polycarbonate box with an open top. At the center of the bottom of the box, there was a hole which was plugged with a rubber septum.

A custom irradiance sensor with a 0.35 mm diameter pierced through the septum into the culture. The sensor was constructed by placing a square cut light guide inside of a 0.35 mm OD steel tube. The flat end of the light guide was placed about 0.2 mm from the opening of the steel tubing and the space between the light guide and the opening of the tube was filled with magnesium oxide powder as a scattering material. A small drop of epoxy adhesive was used to retain the powder.

The irradiance sensor was translated vertically within the algal culture us-

ing a micromanipulator (World Precision Instruments Inc., model M3301R). The sensor was connected via SMA to a spectrometer with a spectral resolution of 1.3 nm (Ocean Optics, USB4000), which was connected to a computer. The SpectraSuite® program from Ocean Optics was used to record the signal from the sensor. A programmable LED array (Telelumen, Light Replicator) was used as the light source.

Irradiance spectra were measured at 8 to 10 depths at increments of 1.0 mm. In all cases, exponential attenuation with depth was observed. The irradiance attenuation coefficient at wavelength λ, α_λ, was then calculated according to,

$$G_\lambda(z)/G_\lambda(0) = e^{-\alpha_\lambda z} \tag{1}$$

where $G_\lambda(z)$ is the spectral irradiance at depth z and $G_\lambda(0)$ is the spectral irradiance just below the culture surface. The value of α_λ was calculated as the value that minimized the sum of squared error (SSE) between Equation (1) and the experimental data. This value was determined using a custom computer program.

The attenuation coefficient was observed to scale linearly with microorganism density. This point will be presented in greater detail in the Results section. The spectral attenuation cross section, A_λ, was thus defined as,

$$A_\lambda = \alpha_\lambda / X \tag{2}$$

where X is the microorganism density in grams of dry biomass per liter (g/l).

2.3.2. Simulation of irradiance at different pond depths

Using the irradiance attenuation coefficients for each culture, α_λ, spectral irradiances at different depths z were calculated according to,

$$G_\lambda(z) = G_\lambda(0)e^{-\alpha_\lambda z} \tag{3}$$

where $G_\lambda(0)$ is the incident spectral irradiance. In these experiments, the incident spectrum was the Direct+Circumsolar spectrum obtained from the National Renewable Energy Laboratory's ASTM G173-03 Reference Spectra resource [34]. This spectrum would be incident onto a pond at noon of the summer solstice at a latitude of 23.4^o.

The irradiance spectra at depths ranging from 0 cm (just below the water surface) to 20 cm were simulated with a programmable LED array (TeleLumen, Light Replicator). The array consisted of LEDs with 16 different peak wavelengths behind a light diffuser 10 cm in diameter. The electrical power input to each color LED could be individually controlled using a custom application (TeleLumen, LumenScripts). For each LED color, a calibration curve between electrical power input and total irradiance was generated using a quantum sensor (Li-Cor, LI-190). The shape of the irradiance spectrum for each LED was reported by the manufacturer. Using these data, a "virtual LED array" program was written in Microsoft Excel which allowed the user to manipulate the electrical power input to each LED until the output spectrum of the entire LED array matched a target spectrum. In this case, the target spectra were the irradiance spectra at different pond depths. These electrical power input settings were then loaded into the LumenScripts application and saved for later use. As a check, the total irradiance between 400

and 700 nm, G_{PAR}, was measured experimentally using a quantum sensor (Li-Cor, LI-190) for several reconstructed spectra. For all of these reconstructions, the measured irradiance was within 10% of the target irradiance designed using the virtual LED array.

2.3.3. Oxygen evolution experiments

Under irradiance spectra corresponding to different pond depths, photosynthetic rate was measured as the time rate of change of dissolved oxygen concentration within an enclosed culture sample. The culture was enclosed in a 1.9 cm deep, 2.5 cm square polycarbonate box with a closed top. The top surface of the box was uniformly illuminated by the LED array. The side of the box had a hole that was plugged with a septum. An optical dissolved oxygen probe (PyroScience, OXR50) pierced through the septum into the culture. A magnetic stirbar was used to keep the sample well mixed to diminish oxygen gradients. After the oxygen probe was inserted, the light was turned on and the dissolved oxygen concentration was measured at a frequency of 1 Hz for about 5 minutes. This time period was selected to be long enough to gather enough data points to calculate an oxygen evolution rate, while not long enough to induce oxygen inhibition of photosynthesis [19]. The net oxygen production rate was calculated using the equation:

$$\frac{dC_{O_2}}{dt} = \overline{\pi}_{O_2} - k_l a \left(C_{O_2} - C_{O_2,h}\right) \tag{4}$$

where C_{O_2} is the dissolved oxygen concentration, t is time, and $\overline{\pi}_{O_2}$ is the average oxygen production rate in the sample, which is the photosynthetic rate minus the respiration rate. The second term on the right hand side accounts for oxygen transfer between the liquid phase and the gas phase,

with $k_l a$ being the mass transfer coefficient between the liquid and the head space of the box and $C_{O_2,h}$ being the oxygen concentration in the head space. This term was introduced as it was experimentally difficult to remove all air from the box.

Equation (4) is a first order linear differential equation with the solution,

$$C_{O_2}(t) = \left(C_{O_2,i} - \frac{\overline{\pi}_{O_2}}{k_l a} - C_{O_2,h} \right) e^{-k_l a t} + \frac{\overline{\pi}_{O_2}}{k_l a} + C_{O_2,h} \tag{5}$$

where $C_{O_2,i}$ is the initial oxygen concentration in the solution. The mass transfer coefficient $k_l a$ was measured experimentally by saturating uninoculated nutrient media with oxygen, purging the head space with nitrogen, and measuring the rate of decrease of dissolved oxygen concentration in the liquid. The value of $k_l a$ was determined to be 0.0018 s^{-1}. A custom curve fitting program was used to determine the net oxygen production rate $\overline{\pi}_{O_2}$. This program looped through values for $\overline{\pi}_{O_2}$ within a specified range at a specified increment, and returned the value that minimized the sum of squared error (SSE) between Equation (5) and experimental data.

2.4. Measurement of the photosynthetic action spectrum

The photosynthetic action spectrum is defined as the photosynthetic rate of an organism as a function of the wavelength of a monochromatic light source [35, 36]. The action spectrum can be measured by measuring oxygen evolution rate under light of various wavelengths, although an action spectrum for the spectral range of 400 to 700 nm at a resolution of 5 nm requires about 10 hours to complete. Alternatively, the action spectrum can be measured by measuring the fluorescence yield from chlorophyll a as a function of

wavelength of an excitation light [36], which requires less than 10 minutes to complete on a plate reader. Chlorophyll a is the reaction center molecule for both green algae and cyanobacteria, so fluorescence from this molecule is an indication that energy from the excitation light was transferred to the reaction center [35]. We measured the photosynthetic action spectra of *Chlorella* and *Spirulina* by measuring the fluorescence yield at 700 nm as a function of excitation wavelength between 400 and 640 nm in a plate reader (Molecular Devices, SpectraMax M5). At wavelengths greater than 640 nm, interference from the excitation light precluded accurate emission yield measurements.

2.5. Biomass densities used for each experiment

To make the pond simulations as realistic as possible, we used the same culture for measurement of attenuation coefficients and oxygen evolution rates. The procedure for measuring attenuation coefficients and oxygen evolution rates for both *Chlorella* and *Spirulina* was as follows: first, the spectral attenuation coefficients of the culture were measured. These attenuation coefficients were used to calculate attenuation cross sections, defined as the attenuation coefficient normalized by the biomass density. These cross sections were then used to calculate the attenuation coefficients for a pond at a target simulated biomass density of 0.19 grams dry biomass per liter (g/l). The irradiance spectra that were reconstructed using these attenuation coefficients were used in the oxygen evolution experiments. The physical culture used in the oxygen evolution experiments was the same culture of which the attenuation coefficients had previously been measured. However, the biomass density of this culture was not necessarily equal to 0.19 g/l. Thus, in the results section, the oxygen evolution rate was normalized by biomass

concentration.

Figure 1 shows the growth curves for the stock cultures of *Chlorella* and *Spirulina*. The arrows represent the times at which experiments were performed. Experiments were performed during exponential growth phase because most biomass production in scaled up ponds occurs during this phase. The uncertainty in biomass density, based on typical standard error between optical density measurements of the same culture, was determined to be 0.01 g/l. For *Chlorella*, attenuation coefficients and oxygen evolution rates were measured at culture ages of 7.0 and 7.3 days, respectively. At both of these times, the biomass density was 0.13 $\pm$ 0.01 g/l. For *Spirulina*, attenuation coefficients and oxygen evolution rates were measured at culture ages of 24 and 25 days, respectively, at which times the biomass density of the physical culture was 1.35 $\pm$ 0.01 g/l, respectively. For oxygen evolution experiments, the *Spirulina* culture was diluted to an experimental biomass density of 0.45 g/l to avoid both nutrient limitation and self shading within the test chamber. Table 1 summarizes the biomass densities that were used for each part of the experiment.

Table 1: Summary of biomass densities used for the experiments (g/l)

	Chlorella	***Spirulina***
Measurement of attenuation coefficients	0.13	1.35
Reconstruction of irradiance spectra	0.19	0.19
Measurement of oxygen evolution rates	0.13	0.45

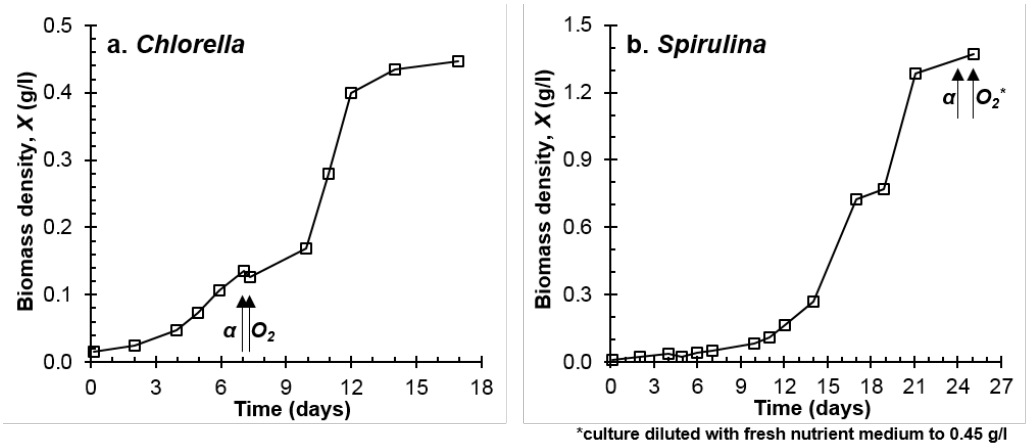

Figure 1: Growth curves for (a) *Chlorella* and (b) *Spirulina*. The α symbols represent the times at which attenuation coefficients were measured. The O_2 symbols represent the time at which oxygen evolution rates were measured.

3. Results and Discussion

3.1. Spectral irradiance attenuation coefficients

Figure 2 shows the irradiance attenuation coefficient as a function of wavelength for *Chlorella* at 0.13 g/l and *Spirulina* at 1.35 g/l. The black curve represents the average of three trials, and the gray curves represent one standard error greater than and less than the average. The standard error was greater for *Spirulina* (about 6.2% on average between 400 and 700 nm) than it was for *Chlorella* (about 1.2%) because increased flocculation in *Spirulina* caused a more heterogeneous microorganism distribution. The attenuation coefficient spectrum of *Chlorella* featured a broad peak spanning from 400 to 500 nm due to absorption by chlorophyll a, chlorophyll b, and carotenoids, with a maximum at 440 nm due to chlorophyll a [37]. Another peak was observed at 680 nm due to chlorophyll a, with a shoulder at 650 nm due

to chlorophyll b. The attenuation coefficient spectrum of *Spirulina* featured a broad peak between 400 and 500 nm due to absorption by chlorophyll a and carotenoids. Absorption by chlorophyll a was also observed at 680 nm. Moreover, absorption by the light harvesting phycobilisome had a peak at 630 nm.

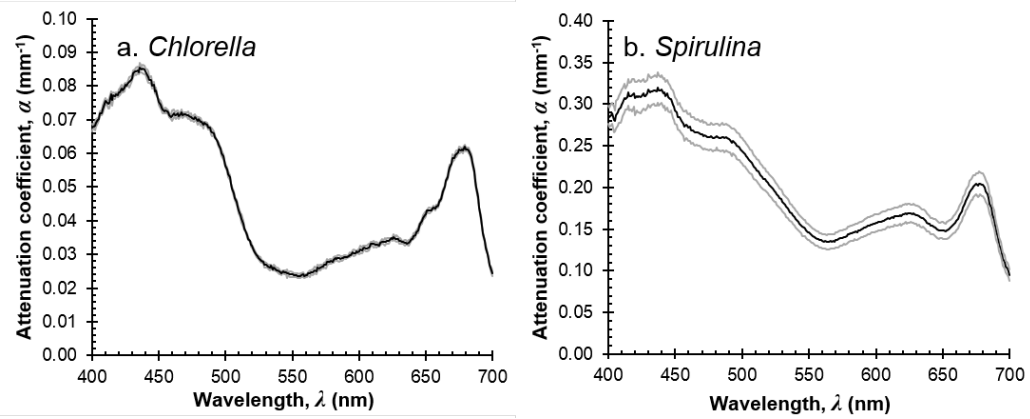

Figure 2: Attenuation coefficients of spectral irradiance in cultures of (a) *Chlorella* at 0.13 g/l and (b) *Spirulina* at 1.35 g/l. Black lines indicate averages of three replicate trials, and gray lines indicate a difference of one standard error.

It is important to note that these attenuation spectra are different from an optical density (absorbance) spectrum measured in a spectrophotometer. In a spectrophotometer, attenuation of a laser beam occurs as absorption and out-scattering remove photons from the beam's path. In contrast, the present experimental setup measures the overall attenuation of downwelling irradiance, which results from absorption and back-scattering of photons traveling in all downward facing directions.

3.2. Attenuation cross sections

The spectral attenuation cross section at wavelength λ, A_λ, was defined as the attenuation coefficient divided by the biomass density. Figure 3a shows the attenuation cross section of four dilutions of the same culture of *Chlorella* with densities ranging from 0.09 to 0.72 g/l, a typical operating range for outdoor raceway ponds [12, 13]. Figure 3b shows the attenuation cross section of five dilutions of the same culture of *Spirulina* with densities ranging from 0.08 g/l to 1.19 g/l. Note that these cultures were different than the cultures whose attenuation coefficients are shown in Figure 2. The main difference between these two sets of cultures is that those shown in Figure 3 were grown indoors under fluorescent lighting, whereas those shown in Figure 2 were grown outdoors under sunlight. Nonetheless, the Figure 3 indicates that the attenuation cross sections of all four dilutions of *Chlorella* were within 19% of each other over the spectral range between 400 and 700 nm. The attenuation cross sections of the dilutions of the *Spirulina* culture were within 27% of each other. These results indicate that the attenuation coefficients of a culture are directly proportional to its biomass density, with an accuracy of about 20% for *Chlorella* between 0.09 and 0.72 g/l, and an accuracy of about 30% for *Spirulina* between 0.08 and 1.19 g/l. Therefore, if the biomass concentration of a culture is known to be X_c, its attenuation coefficients can be calculated by multiplying the attenuation coefficients shown in Figure 2 by the factor X_c/X_α, where X_α is the biomass density of the cultures presented in Figure 2.

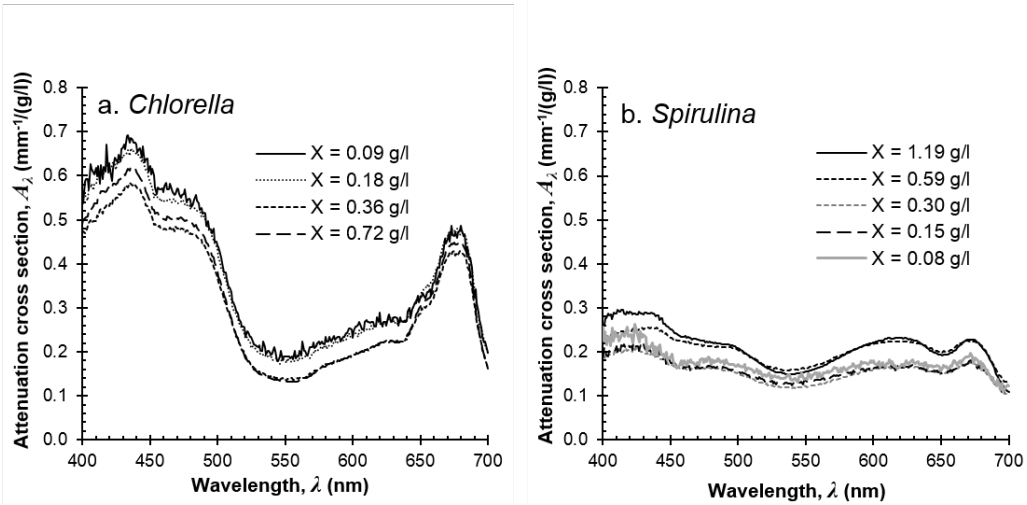

Figure 3: Attenuation cross section, defined as the attenuation coefficient divided by the microorganism density, for (a) four dilutions of the same culture of *Chlorella* ranging from 0.09 to 0.72 g/l, and (b) five dilutions of one culture of *Spirulina* ranging from 0.08 to 1.19 g/l. Note that these cultures are different from the cultures presented in Figure 2.

3.3. Simulation of irradiance spectra at different pond depths

Using the attenuation cross sections presented in Figure 3, a programmable LED array was used to simulate the irradiance spectra at different depths within ponds of *Chlorella* and *Spirulina* at 0.19 g/l. Figure 4 shows example comparisons between the target and simulated irradiance spectra for incident sunlight as well as at depths of 4 cm and 10 cm in these ponds. Agreement was generally good between the target and simulated spectra. One exception occurred near 680 nm, which occurred because the LED array lacked LEDs with peak emission near this wavelength. Chlorophyll a absorbs maximally at 680 nm, so it is expected that the photosynthetic rate would be slightly lower under the simulated spectrum than under the target spectrum. This

spectral mismatch at 680 nm became less of an issue at depths greater than 2 cm, where the target spectrum was also depleted of light in this spectral band due to chlorophyll absorption.

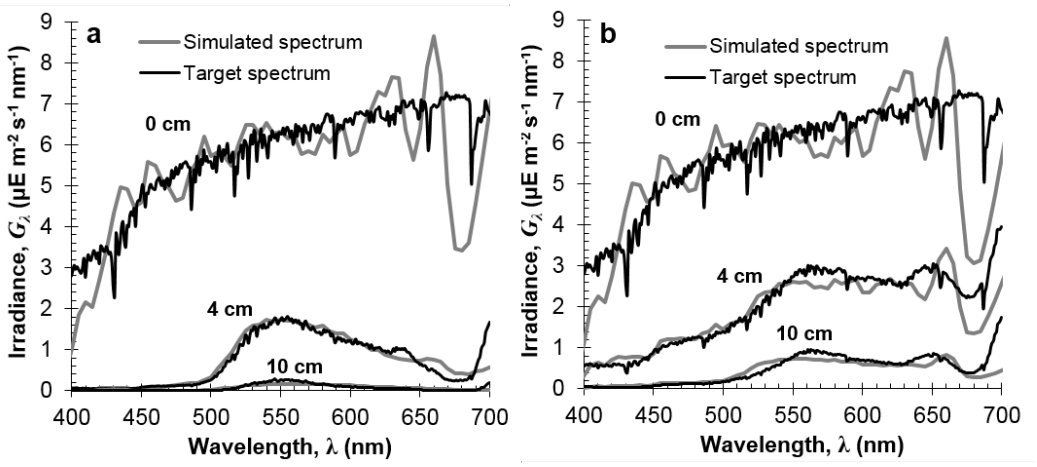

Figure 4: Target irradiance spectra and spectra simulated by the programmable LED array at different depths within open ponds of (a) *Chlorella* and (b) *Spirulina*.

3.4. Photosynthetic rate as a function of simulated depth

Figure 5a shows the net oxygen evolution rate , $\overline{\pi}_{O_2}$, as a function of depth within a simulated pond of *Chlorella* at 0.19 g/l. The oxygen evolution rate is presented in units of μmol O_2 per gram of dry biomass per second (μmol/g-s). The depth of each point in the figure, z, was calculated as

$$z = z_p + (h_b/2)(X_{O_2}/X_p) \tag{6}$$

where z_p is the depth for which the irradiance spectrum was designed, h_b is the thickness of the culture sample, equal to 1.9 cm, and X_{O_2} and X_p are the biomass concentrations used in the O_2 evolution experiments and for the

spectrum construction, respectively. Conceptually, this depth corresponds to the midpoint of the culture sample, corrected for the fact that the biomass concentrations in the O_2 evolution experiments were different than those simulated by the depth spectra. For *Chlorella*, the oxygen evolution rate decreased from 1.1 μmol/g-s at the smallest tested depth of 0.7 cm to 0 μmol/g-s at a depth of 12 cm (Figure 5a). This depth, at which the rates of photosynthesis and respiration were equal, is referred to as the compensation depth. At the compensation depth the total irradiance between 400 and 700 nm (G_{PAR}) was 9 μmol photons/m^2-s. However, as shown in Figure 4a, this irradiance predominantly had wavelengths in the green region between 500 to 600 nm, and *Chlorella* does not have pigments that effectively utilize light in this spectral band [22, 23]. At depths greater than 12 cm, net oxygen production was negative due to respiration. In fact, the magnitude of the total oxygen consumption below the compensation depth was equal to about 15% of the total oxygen production above it.

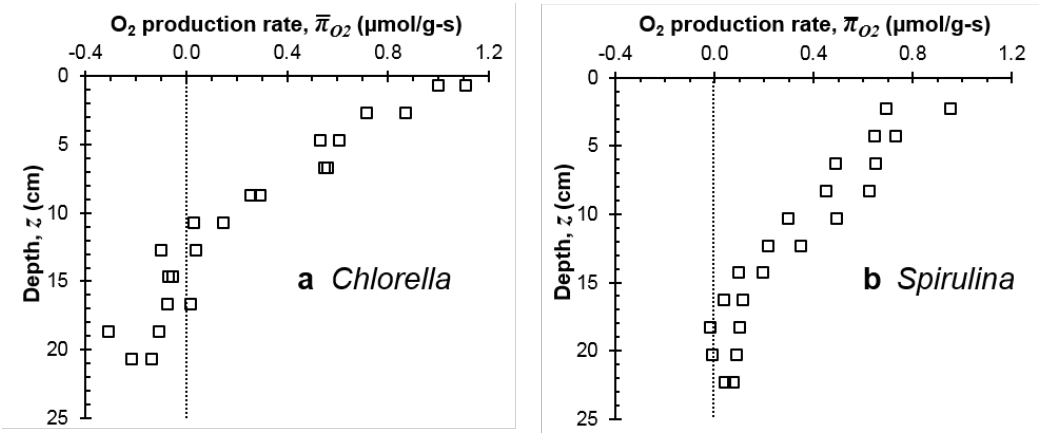

Figure 5: Net oxygen production rate in simulated ponds of (a) *Chlorella* and (b) *Spirulina* at a biomass density of 0.19 g/l.

Figure 5b shows the depth dependence of oxygen evolution in the simulated pond of *Spirulina* at 0.19 g/l. The net oxygen evolution rate decreased from 0.82 μmol/g-s at the smallest tested depth of 2.3 cm to an average of 0.06 μmol/g-s in the depth range between 16 cm and 23 cm. At a depth of 16 cm, the total irradiance was 37 μmol photons/m^2-s. Significant respiration (on the order of 10% of maximum oxygen production) was not observed in the simulated *Spirulina* pond.

The oxygen evolving region in the simulated *Spirulina* pond was thicker than that in the *Chlorella* pond partly because light capable of supporting oxygen production was able to penetrate deeper into the *Spirulina* culture. The attenuation cross section, averaged over the range of 400 to 700 nm, was 0.35 mm^{-1}/(g/l) for *Chlorella*, whereas it was only 0.15 mm^{-1}/(g/l) for *Spirulina*. This difference is likely due to the sieve effect [38]. The propensity of *Spirulina* to flocculate causes some light paths through the culture to be unimpeded by organisms, whereas other light paths are significantly impeded by clumps. The overall effect is to increase the overall transmittance of the culture.

3.5. Effect of light regime on photosynthetic rate

In the simulated *Chlorella* and *Spirulina* ponds, the net oxygen production rate approached zero at depths of about 12 cm and 16 cm, respectively. Productivity decreased with increasing depth as a result of, first, attenuation of the total irradiance, and second, variation in the spectral content of the irradiance. It is of interest in this section to compare the relative importance of these two effects.

To quantify the effect of spectral content of irradiance on photosynthetic

productivity, we employ a method similar to that proposed by Morel [39], Kyewalyanga *et al.* [40], and Markager and Vincent [41]. In these studies, a spectral matching parameter was defined as the degree of overlap between the absorption spectrum of an alga and the irradiance spectrum incident upon it. Thus, a monochromatic light source at the wavelength of maximum algal absorptivity would have a spectral matching value of 1, whereas monochromatic light at a wavelength at which the alga was completely non-absorbing would have a spectral matching parameter value of 0. It was shown that the product of the spectral matching parameter and the total irradiance between 400 and 700 nm (G_{PAR}) more precisely controls photosynthetic rate than does the G_{PAR} itself [41]. The photosynthetically *useful* irradiance, G_{PU}, can therefore be defined as,

$$G_{PU}(z) = S(z)G_{PAR}(z) \tag{7}$$

where $S(z)$ is the spectral matching parameter at depth z. In this study, we define the spectral matching parameter as the overlap between a local (depth-dependent) irradiance spectrum and the action spectrum of the organism:

$$S(z) = \frac{\int_{400nm}^{700nm} a_\lambda G_\lambda(z) d\lambda}{\int_{400nm}^{700nm} G_\lambda(z) d\lambda} \tag{8}$$

where a_λ is the photosynthetic action spectrum value of the microorganisms at wavelength λ, normalized to a scale of 0 to 1. This matching parameter differs from those used previously [39–41] in that it takes into account the action spectrum of the organisms, which describes their photosynthetic response to light at a particular wavelength, rather than their absorption

spectrum, which does not take into account the spectral variation in photosynthetic efficiency.

Figure 6 shows the action spectra a_λ of *Chlorella* and *Spirulina*. Due to equipment limitations, it was not possible to measure the action spectra values at wavelengths greater than 650 nm. However, the measured action spectra for *Chlorella* and *Spirulina* at wavelengths below 650 nm showed good agreement with the action spectra reported by McLeod [35] for the green alga *Chlorella pyrenoidosa* and the cyanobacterium *Anacystis nidulans*, respectively. Therefore, values for wavelengths between 650 nm and 700 nm were selected based on values from McLeod [35]. The action spectra presented in Figure 6 should thus be considered a semi-quantitative data set primarily for the purpose of illustration. The action spectrum of *Chlorella* showed peaks at 440 nm and 680 nm, 480 and 660 nm, and 450 to 500 nm, corresponding to absorption by chlorophyll a, chlorophyll b, and carotenoids, respectively [37]. On the other hand, *Spirulina* had only one action spectrum peak at 610 nm, corresponding to absorption by the light-harvesting phycobilisome [42].

It is important to note that for *Chlorella*, the shapes of the action spectrum and attenuation coefficient spectrum are very similar, whereas for *Spirulina* they are quite different. This is a general difference between green algae and cyanobacteria. In both green algae and cyanobacteria, a light harvesting complex is responsible for absorbing radiant energy and delivering it to the photosynthetic reaction center [42, 43]. Both green algae and cyanobacteria utilize chlorophyll a as their reaction center pigment. However, green algae have a light harvesting complex consisting mostly of chlorophyll, whereas

the light harvesting complex in cyanobacteria consists of phycobiliproteins, which absorb in the spectral region between 550 and 650 nm. The action spectra of *Chlorella* and *Spirulina* therefore represent the absorption spectra of their respective light harvesting complexes.

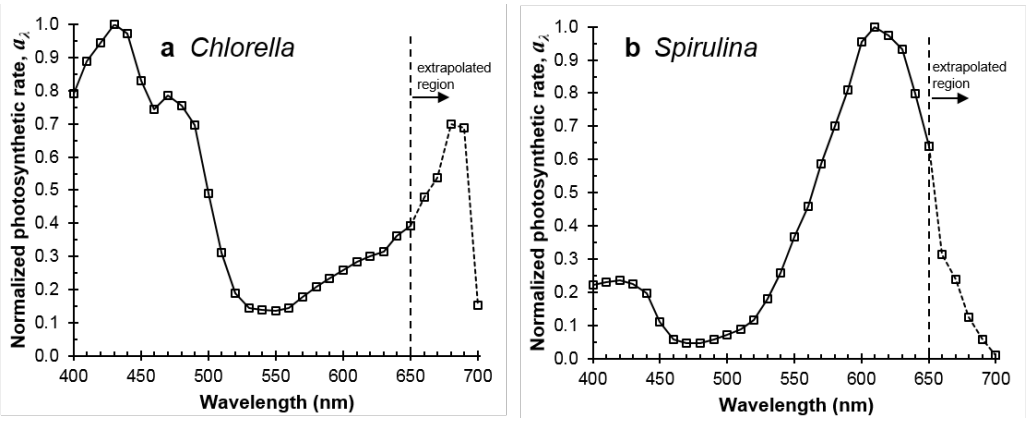

Figure 6: Action spectra for (a) *Chlorella* and (b) *Spirulina* measured by fluorescence emission yield at 700 nm as a function of excitation wavelength. Values in the extrapolated region were selected based on the spectra reported by McLeod [35], which showed good agreement with the spectra measured in the current study for wavelengths less than 650 nm.

Figure 7 shows the variation of the spectral matching parameter S with simulated pond depth for *Chlorella* and *Spirulina* illuminated by a solar spectrum. The matching parameter for *Chlorella* decreased from 0.44 for incident solar radiation to 0.24 at a depth of 6 cm, and then gradually approached an asymptotic value of about 0.16 with increasing depth. For *Spirulina*, the matching parameter actually increased with depth in the culture, from a value of 0.40 for full sunlight toward an asymptotic value of about 0.50. This increase occurred because the irradiance in the blue region (between 400 and 500 nm) decreased rapidly with depth in the *Spirulina* culture, and oxygen

production by *Spirulina* is relatively low in this spectral region (Figure 6b).

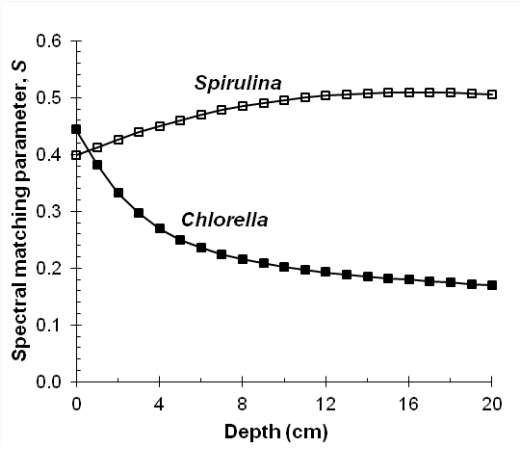

Figure 7: Variation of the spectral matching parameter with depth in 20 cm deep cultures of (a) *Chlorella* at 0.18 g/l and *Spirulina* at 0.19 g/l.

Over the depth of a 20 cm deep pond, the spectral matching parameters for *Chlorella* and *Spirulina* decreased by a factor of about 2.8 and increased by a factor of 1.3, respectively. These variations in spectral matching parameters were small compared to the variation in total irradiance between 400 and 700 nm (G_{PAR}). Using the virtual LED array program, we calculated that the ratio of total G_{PAR} at the surface to the total G_{PAR} at a depth of 20 cm was 3,400 in the *Chlorella* pond and 110 in the *Spirulina* pond. Given that the magnitude and spectral quality contribute equally to the photosynthetically useful irradiance (Equation 7), decreasing productivity with increasing depth in open ponds is predominantly due to attenuation of the magnitude of the irradiance with increasing depth, with variation in spectral content playing a minor role.

3.6. Implications for scaled up open pond design

For the simulated pond of *Chlorella* at 0.19 g/l, the total oxygen consumption by cells below the compensation depth had a magnitude of about 15% that of the oxygen production above the compensation depth. Moreover, the biomass concentration of 0.19 g/l in these experiments was less than a typical operating biomass concentration of about 0.3 g/l [5, 13]. It has been shown in this study that irradiance is attenuated exponentially with depth, and that the coefficient of exponential attenuation is proportional to biomass concentration. It then follows that the compensation depth will scale inversely with the biomass concentration. Therefore, an increase in culture density from 0.19 g/l to 0.3 g/l is expected to be accompanied by a decrease in the compensation depth from 12 cm to about 7 cm. It is also expected that the ratio of respiration to photosynthesis in a pond with a concentration of 0.3 g/l would be greater than the 15% observed here.

Significant net oxygen consumption was not observed at any simulated depth in the *Spirulina* pond, although the top 12 cm of the pond accounted for 93% of the overall productivity. Using the same argument as above, an increase in biomass concentration from the 0.19 g/l used in this study to a more typical 0.3 g/l would be expected to decrease the depth of this productive region from 12 cm to about 7 cm. Given the depth resolution of pond productivity observed in this study, it is therefore recommended that the depth of open raceway ponds be decreased to about 10 cm to enhance productivity.

It has been observed that shallower ponds achieve greater biomass densities [12, 15]. Therefore, in practice, the overall effect of decreasing the depth

of a pond from 20 cm to 10 cm would likely be an an approximate doubling the operating biomass density, with the ratio of the photic zone depth to the overall pond depth remaining roughly constant. This increase in biomass density would manifest itself as a decrease in energetic and monetary costs of dewatering and harvesting the resultant biomass. This strategy has been employed in Czech reactors [15].

Decreasing pond depth also reduces the input power required to circulate fluid through the pond. This power requirement, $\dot{W}$, can be written as [44],

$$\dot{W} = vdw\Delta P \tag{9}$$

where v is the average flow velocity, w is the width of a pond cross section, d is the depth, and ΔP is the pressure drop over one track length. Therefore, halving the pond depth while leaving pond width and flow velocity constant reduces the power consumption by about half. The pressure drop ΔP would also decrease, but this would have a lesser effect on $\dot{W}$ because the wetted surface area of most ponds is dominated by the bottom rather than the sides [12].

While areal productivity increases and harvesting and operating costs decrease upon making ponds shallower, capital costs increase due to the following argument. As fluid circulates around a raceway pond, its pressure decreases due to friction with the pond walls. This pressure drop is manifested as a drop in water column height with increasing distance along the track, making the pond shallower at the end of the track than at the beginning. The paddle wheel serves to lift the fluid, which sustains flow around the track. Decreasing the average depth of a pond from 20 cm to 10 cm de-

creases the pond depth at the end of the track, which decreases the amount of fluid that the paddle wheel can lift. To compensate for the lesser head that can be provided by the paddle wheel, the raceway must be made shorter to decrease the frictional pressure drop. Therefore, a greater number of shallower ponds would need to be constructed to cover the same footprint area as fewer deeper ones. Using a mathematical methodology described by Oswald [10], Borowitzka [12] calculated that for a flow velocity of 0.3 m/s and a pond width of 6 m, a 10 cm deep pond would have a maximum area of about 0.07 hectares, compared to a maximum area of 0.32 hectares for a 20 cm deep pond. Thus, about nine shallower ponds would need to be built instead of two deeper ponds to cover the same footprint area. The details of these calculations are provided as supplementary material.

It has also been proposed that the presence of a pond region below the compensation depth can actually increase, rather than decrease, overall productivity. Specifically, it has been argued that cells are most productive when they are shuttled between the photic and aphotic zones [14, 45]. This is known as the "flashing light effect." However, the literature presents conflicting evidence as to whether the flashing light effect increases productivity when the frequency of flashing corresponds to turnover times of seconds to minutes, which would be expected in an open pond [46–49].

Finally, decreasing the depth of a pond decreases its thermal mass, which increases its diurnal and seasonal range of temperature fluctuation [14, 50]. Ponds can become warmer than the ambient air during the day due to solar heating, and colder than ambient air at night due to evaporative cooling. The magnitude of the difference between the pond temperature and the air

temperature is inversely related to depth [50]. A shallower pond therefore has an increased time-averaged difference between pond temperature and optimal algal growth temperature, which acts to decrease the time-averaged growth rate. However, the total decrease in time-averaged growth rate due to increased temperature fluctuation will be dependent on both environmental conditions and algal growth kinetics.

Designing open pond raceways for maximum return on investment requires careful quantitative consideration of the effect of pond depth on areal productivity, paddle wheel input power, dewatering and harvesting costs, and capital costs. This work provides experimental data for algal productivity as a function of depth within simulated open ponds, which can in turn be used to predict total productivity as a function of overall pond depth. In addition to quantitative assessments of the dependence of pond depth on operating and capital costs, this work can serve as a tool to optimize the geometric design of open ponds.

4. Conclusions

We have presented cross sections of photosynthetic productivity as a function of simulated depth within 20 cm deep open pond raceways of *Chlorella vulgaris* and *Spirulina platensis* at a biomass concentration of 0.19 grams of dry biomass per liter (g/l). To simulate depth, we reproduced the magnitude and spectral composition of irradiance at various depths within these ponds using a programmable LED array. Photosynthetic productivity was measured as oxygen evolution rate. Results indicated that the compensation depth, or the depth at which net oxygen production was equal to zero, was

12 cm for *Chlorella* at 0.19 g/l. Net oxygen production was positive at all depths in the *Spirulina* pond at 0.19 g/l, although 90% of the oxygen was produced by the top 13 cm of the pond. From the perspective of maximizing productivity, ponds should be designed shallower than the conventional 20 cm by at least a factor of two. However, it is acknowledged that making a pond shallower decreases its maximum potential footprint area due to hydraulic limitations, potentially increasing capital costs for hectare scale algal farms. It is recommended that a careful optimization analysis be performed which takes into account the effect of pond depth on the costs of initial algal farm construction, paddle wheel power input, and dewatering and harvesting costs, as well as on biomass productivity. This paper provides quantitative data on the effect of pond depth on productivity for such an optimization study.

Acknowledgements

The authors would like to thank Sue Carter at UC-Santa Cruz for the lease of the Telelumen LED array. The authors are also grateful for the funding provided by the NASA Postdoctoral Program, the NASA Internship Program, and the Cornell Tradition Fellowship. We would also like to sincerely thank two anonymous reviewers, whose comments significantly improved the manuscript.

References

[1] P. Spolaore, C. Joannis-Cassan, E. Duran, and A. Isambert, "Commercial applications of microalgae", *J Biosci Bioeng*, vol. 101, no. 2, pp.

87–96, 2006.

[2] J.J. Milledge, "Commercial application of microalgae other than as biofuels: a brief review", *Rev Env Sci Biotechnol*, vol. 10, no. 1, pp. 31–41, 2010.

[3] J.R. Benemann, "Microalgae aquaculture feeds", *J Appl Phycol*, vol. 4, no. 3, pp. 233–245, 1992.

[4] D.E. Brune, T.J. Lundquist, and J.R. Benemann, "Microalgal biomass for greenhouse gas reductions: potential for replacement of fossil fuels and animal feeds", *J Environ Eng*, vol. 135, no. 11, pp. 1136–1144, 2009.

[5] C.M. Beal, L.N. Gerber, D.L. Sills, M.E. Huntley, S.C. Machesky, M.J. Walsh, J.W. Tester, I. Archibald, J. Granados, and C.H. Greene, "Algal biofuel production for fuels and feed in a 100-ha facility: A comprehensive techno-economic analysis and life cycle assessment (in press)", *Algal Res*, 2015.

[6] P.T. Pienkos and A. Darzins, "The promise and challenges of microalgal-derived biofuels", *Biofuel Bioprod Bior*, vol. 3, pp. 431–440, 2009.

[7] A.F. Clarens, E.P. Resurreccion, M.A. White, and L.M. Colosi, "Environmental life cycle comparison of algae to other bioenergy feedstocks", *Environ Sci Technol*, vol. 44, no. 5, pp. 1813–1819, 2010.

[8] S.A. Scott, M.P. Davey, J.S. Dennis, I. Horst, C.J. Howe, D.J. Lea-Smith, and A.G. Smith, "Biodiesel from algae: challenges and prospects.", *Curr Opin Biotechnol*, vol. 21, no. 3, pp. 277–86, 2010.

[9] Y. Chisti and J. Yan, "Energy from algae: Current status and future trends", *Appl Energ*, vol. 88, no. 10, pp. 3277–3279, 2011.

[10] W.J. Oswald, "Large-scale algal culture systems (engineering aspects)", in *Micro-Algal Biotechnology*, M.A. Borowitzka and L.J. Borowitzka, Eds., pp. 357–394. Cambridge University Press, Cambridge, 1988.

[11] M.A. Borowitzka, "Commercial production of microalgae: ponds, tanks, tubes, and fermenters.", *J Biotechnol*, vol. 70, pp. 313–321, 1999.

[12] M. Borowitzka, "Culturing microalgae in outdoor ponds", in *Algal Culturing Techniques*, R.A. Andersen, Ed., pp. 205–218. Elsevier, 2005.

[13] O. Jorquera, A. Kiperstok, E.A. Sales, M Embiruçu, and M.L. Ghirardi, "Comparative energy life-cycle analyses of microalgal biomass production in open ponds and photobioreactors.", *Bioresource Technol*, vol. 101, no. 4, pp. 1406–1413, 2010.

[14] "Mass Cultivation of Phototrophic Algae", in *Recent Advances in Microalgal Biotechnology*, Jin Liu, Zheng Sun, and Henri Gerken, Eds. OMICS Ebooks Group, Foster City, CA, 2014.

[15] J. Doucha and K. Lívanský, "Outdoor open thin-layer microalgal photobioreactor: potential productivity", *J Appl Phycol*, vol. 21, pp. 111–117, 2009.

[16] M.L. Shuler and F. Kargi, *Bioprocess engineering, basic concepts*, Prentice-Hall, Upper Saddle River, NJ, USA, 2nd edition, 2002.

628 [17] R.J. Craggs, S. Heubeck, T.J. Lundquist, and J.R. Benemann, "Algal
629 biofuels from wastewater treatment high rate algal ponds", *Water Sci*
630 *Technol*, vol. 63, no. 4, pp. 660–5, 2011.

631 [18] Y. Jeon, C. Cho, and Y. Yun, "Measurement of microalgal photosyn-
632 thetic activity depending on light intensity and quality", *Biochem Engin*
633 *J*, vol. 27, no. 2, pp. 127–131, 2005.

634 [19] C. Brindley, F.G. Acien, and J.M. Fernandez-Sevilla, "The oxygen
635 evolution methodology affects photosynthetic rate measurements of mi-
636 croalgae in well-defined light regimes", *Biotechnol Bioeng*, vol. 106, no.
637 2, pp. 228–237, 2010.

638 [20] R.J. Ritchie and A.W.D. Larkum, "Modelling photosynthesis in shallow
639 algal production ponds", *Photosynthetica*, vol. 50, pp. 481–500, 2012.

640 [21] R.E. Lee, *Phycology*, Cambridge University Press, Cambridge, fourth
641 edition, 2008.

642 [22] R.R. Bidigare, M.E. Ondrusek, J.H. Morrow, and D.A. Kiefer, "*In vivo*
643 absorption properties of algal pigments", *SPIE*, vol. 1302, pp. 290–302,
644 1990.

645 [23] R.A. Andersen, *Algal Culturing Techniques*, Elsevier Academic Press,
646 London, 2005.

647 [24] Y. Chisti, "Biodiesel from algae", *Biotechnol Adv*, vol. 25, pp. 294–306,
648 2007.

649 [25] O. Pulz and W. Gross, "Valuable products from biotechnology of mi-
650 croalgae", *Appl Microbiol Biot*, vol. 65, no. 6, pp. 635–648, 2004.

651 [26] M. Görs, R. Schumann, D. Hepperle, and U. Karsten, "Quality analysis
652 of commercial Chlorella products used as dietary supplement in human
653 nutrition", *J Appl Phycol*, vol. 22, no. 3, pp. 265–276, 2009.

654 [27] A. Vonshak, Ed., *Spirulina Platensis (Arthrospira): Physiology, Cell-
655 biology and Biotechnology*, CRC Press, Boca Raton, FL, 1997.

656 [28] P. Nomsawai, N.T. DeMarsac, J.C. Thomas, M. Tanticharoen, and
657 S. Cheevadhanarak, "Light regulation of phycobilisome structure and
658 gene expression in *Spirulina platensis* C1 (*Arthrospira* sp PCC 9438)",
659 *Plant Cell Physiol*, vol. 40, no. 12, pp. 1194–1202, 1999.

660 [29] F.W. Teale and R.E. Dale, "Isolation and spectral characterization of
661 phycobiliproteins", *Biochem J*, vol. 116, pp. 161–169, 1970.

662 [30] C. Lemasson, N.T. Marsac, and G. Cohen-Bazire, "Role of allophyco-
663 cyanin as light-harvesting pigment in cyanobacteria", *PNAS*, vol. 70,
664 no. 11, pp. 3130–3133, 1973.

665 [31] A. Richmond, E. Lichtenberg, B. Stahl, and A. Vonshak, "Quantita-
666 tive assessment of the major limitations on productivity of *Spirulina
667 platensis* in open raceways", *J Appl Phycol*, vol. 2, pp. 195–206, 1990.

668 [32] U.G. Schlösser, "Sammlung von Algenkulturen", *Berichte der
669 Deutschen Botanischen Gesellschaft*, vol. 95, pp. 181–276, 1982.

[33] A.M. Detweiler, C.E. Mioni, K.L. Hellier, J.J. Allen, S.A. Carter, B.M. Bebout, E.E. Fleming, C. Corrado, and L.E. Prufert-Bebout, "Evaluation of wavelength selective photovoltaic panels on microalgae growth and photosynthetic efficiency", *Algal Research*, vol. 9, pp. 170–177, 2015.

[34] C.A. Gueymard, D. Myers, and K. Emery, "Proposed reference irradiance spectra for solar energy system testing", *Sol Energy*, vol. 73, no. 6, pp. 443–467, 2002.

[35] G.C. McLeod, "Delayed light action spectra of several algae in visible and ultraviolet light", *J Gen Physiol*, vol. 42, no. 955, pp. 243–250, 1958.

[36] M.R. Lewis, O. Ulloa, and T. Platt, "Photosynthetic action, absorption, and quantum yield spectra for a natural population of *Oscillatoria* in the North Atlantic", *Limnol Oceanogr*, vol. 33, no. 1, pp. 92–98, 1988.

[37] M. Stomp, J. Huisman, L.J. Stal, and H.C.P. Matthijs, "Colorful niches of phototrophic microorganisms shaped by vibrations of the water molecule", *ISME J*, vol. 1, pp. 271–282, 2007.

[38] L. Fukshansky, A.M.V. Remisowsky, J. McClendon, A. Ritterbusch, T. Richter, and H. Mohr, "Absorption spectra of leaves corrected for scattering and distributional error: a radiative transfer and absorption statistics treatment", *Photochem Photobiol*, vol. 57, pp. 538–555, 1993.

[39] A. Morel, "Available, usable, and stored radiant energy in relation to marine photosynthesis", *Deep Sea Res*, vol. 25, pp. 673–688, 1978.

[40] M.N. Kyewalyanga, T. Platt, and S. Sathyendranath, "Estimation of the photosynthetic action spectrum: implication for primary production models", *Mar Ecol Prog Ser*, vol. 146, pp. 207–223, 1997.

[41] S. Markager and W.F. Vincent, "Light absorption by phytoplankton: development of a matching parameter for algal photosynthesis under different spectral regimes", *J Plankton Res*, vol. 23, pp. 1373–1384, 2001.

[42] D. Campbell, V. Hurry, A.K. Clarke, P. Gustafsson, and G. Öquist, "Chlorophyll fluorescence analysis of cyanobacterial photosynthesis and acclimation", *Microbiol Mol Biol R*, vol. 62, no. 3, pp. 667–83, 1998.

[43] R.E. Blankenship, *Molecular Mechanisms of Photosynthesis*, Blackwell Science Ltd., Oxford, 2002.

[44] F.M. White, *Viscous Fluid Flow*, McGraw-Hill, New York, third edition, 2006.

[45] J.A. Grobbelaar, "Mass Production of Microalgae at Optimal Photosynthetic Rates", in *Photosynthesis*. InTech, 2013.

[46] J.U. Grobbelaar, "Turbulence in mass algal cultures and the role of light/dark fluctuations", *J Appl Phycol*, vol. 6, pp. 331–335, 1994.

[47] N.J. Kim, I.S. Suh, B.K. Hur, and C.G. Lee, "Simple monodimensional model for linear growth rate of photosynthetic microorganisms in flat-plate photobioreactors", *J Microbiol Biotechnol*, vol. 12, pp. 962–971, 2002.

[48] E. Sforza, D. Simionato, G.M. Giacometti, A. Bertucco, and T. Morosinotto, "Adjusted light and dark cycles can optimize photosynthetic efficiency in algae growing in photobioreactors", *PLoS ONE*, vol. 7, no. 6, 2012.

[49] D.L. Sutherland, V. Montemezzani, C. Howard-Williams, M.H. Turnbull, P.A. Broady, and R.J. Craggs, "Modifying the high rate algal pond light environment and its effects on light absorption and photosynthesis", *Water Res*, vol. 70, pp. 86–96, 2015.

[50] T.E. Murphy and H. Berberoglu, "Temperature fluctuation and evaporative loss rate in an algae biofilm photobioreactor.", *J Sol Energ-T ASME*, vol. 134, pp. 011002–1–011002–9, 2012.